American Mineralogist, Volume 70, pages 1114–1126, 1985

Mineralogy and partial melting of fenitized crustal xenoliths in the Oldoinyo Lengai carbonatitic volcano, Tanzania

VIORICA MOROGAN[1] AND ROBERT F. MARTIN

Department of Geological Sciences
McGill University, 3450 University Street
Montreal, Quebec, Canada H3A 2A7

Abstract

Progressive stages of fenitization are recorded in nine xenoliths of metagranitic and metagabbroic basement that were caught up in alkali carbonatitic magma in the Oldoinyo Lengai volcano, Gregory Rift, Tanzania. The ultimate product of fenitization of the two rock types contains sanidine, nepheline and aegirine-augite. Temperatures of approximately 800°C were attained during metasomatism. Disequilibrium melting of the highest-grade assemblages occurred along grain margins, followed by a rapid quench, which prevented homogenization of melt compositions and devitrification. Such anatectic reactions involving a strongly metasomatized lower crust may be responsible for the juxtaposition of phonolitic and alkali carbonatitic melts with mantle-derived nephelinitic magmas at Oldoinyo Lengai.

Introduction

Fenitization refers to the sum of metasomatic adjustments that bring a country rock into compositional equilibrium with an alkali silicate or carbonatite intrusive complex. These adjustments result from the interaction of country rocks with a peralkaline fluid that emanates from the cooling igneous body. In almost all cases, the high-temperature mineral assemblages that develop re-equilibrate extensively at lower temperatures. Thus fenites typically contain ordered, virtually end-member K- and Na-feldspars instead of a single, disordered (Na,K) feldspar. The efficiency of the retrograde reactions can be attributed to the reactivity of the fluid medium and of the minerals in contact with it.

If the metasomatic transformations occur at a sufficiently high temperature, the metasomatic assemblages will be involved in melting reactions. Direct proof that melting had occurred could only come from the preservation of glass in fenites. Fenitized blocks that had begun to melt would have to be quenched rapidly, as xenoliths in erupted magma, so that the glass could survive metastably. We describe here the fenitic assemblages developed in nine xenoliths of basement granite and gabbro caught up in alkali carbonatitic magma in the Oldoinyo Lengai volcano, in the Gregory Rift, Tanzania. The high-grade fenitic assemblages show clear signs of incipient melting. Such reactions may be regionally important in the lower crust and uppermost mantle beneath continental rift zones.

The regional context

The currently active Oldoinyo Lengai nephelinitic-carbonatitic volcano is the most recent manifestation of a cycle of alkaline magmatism that has affected the southern extremity of the Gregory Rift since Plio-Pleistocene times (Le Bas, 1980). A secular change has occurred in the eruptive style of Oldoinyo Lengai and in the magma types extruded, from quiescent outpourings of alkali basalt and olivine-rich nephelinite to highly explosive manifestations of nephelinitic–phonolitic–carbonatitic volcanism. The locus of modern basaltic volcanism has migrated eastward, to the Kilimanjaro area. The Tanzanian sector of the Gregory Rift (Fig. 1) is the only place in the East African magmatic province where the alkali basalt–olivine nephelinite and nephelinite–carbonatite associations are juxtaposed (Le Bas, 1977).

The rocks exposed near Oldoinyo Lengai are the products of the basalt–nephelinite phase of volcanism. These flows were extruded directly onto the Precambrian basement, now concealed. Basement rocks, exposed to the west and east of the rift zone (Fig. 1), consist of granitic and migmatitic rocks of the Tanzanian Shield and metamorphic rocks of the Mozambique orogenic belt (Guest, 1954; Pickering, 1961). The only basement rocks noted in the early literature on Oldoinyo Lengai were found as ejected blocks of granitic gneiss in the older, southern crater (Reck, 1914). This area was totally covered by a blanket of pyroclastic material in 1917.

Although mainly characterized by pyroclastic deposits, Oldoinyo Lengai is best known for its outpouring of alkali carbonatite lava and ash (Dawson et al., 1968). In addition to fragments of nephelinite and phonolite, which predominate, the pyroclastic material contains nodules of ijolite, nepheline syenite, biotite pyroxenite, fenite and sövite. This array of lithologies suggests the existence at depth of an alkaline suite and related metasomatic rocks. The ubiquity of the fenite blocks throughout the stratigraphic sequence of pyroclastic material (Dawson, 1962) suggests that the alkali metasomatism is early and widespread.

Our study is based on nine xenoliths developed at the expense of two distinct original lithologies: granitic gneiss

[1] Present address: Geologiska Institutionen, Stockholms Universitet, Box 6801, S-113 86 Stockholm, Sweden.

0003–004X/85/1112–1114$02.00

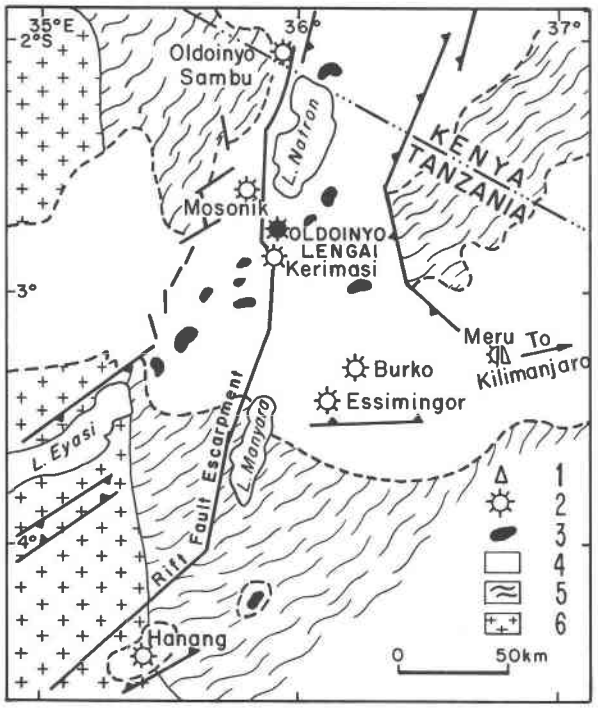

Fig. 1. Geological and tectonic setting of Oldoinyo Lengai volcano (based on the 1:2,000,000 geological map of Tanzania, published in 1959). 1 alkali basalt volcanos (Pleistocene to Recent), 2 nephelinite–carbonatite volcanos (Pleistocene to Recent), 3 alkali basalt–olivine nephelinite volcanos (Pliocene), 4 Tertiary volcanic rocks, 5 Mozambique belt, 6 granitic Tanzanian shield.

and metagabbro. It must be viewed as a first attempt to document the assemblages developed. These have been classified into low-, medium- and high-grade types on the bases of mineral assemblages and textures.

Table 1. Modal composition of fenite xenoliths, Oldoinyo Lengai

	BD58	BD44	BD32	BD48	BD43	BD42	BD35	BD55
alkali feldspar	63		38	47	46	7	58	51
plagioclase	4	33					28	35
clinopyroxene	20	21	34	40	28	51	3	1
hornblende		34						
biotite	1	5						
quartz	1.5		2					
wollastonite	7		8	5	1		6*	8*
calcite	2.5	2	5	4			2	2
opaque phases	1	3			8	4		
apatite	tr	1	2	1	2	2		
titanite		1	1	3	3	6	1	tr
nepheline					5	30		
melanite							tr	1
glass					7	tr	2	2
number of points counted	1200	1000	1200	1000	400	700	600	500

BD58 low-grade fenite, granitic gneiss ancestor; BD44 low-grade fenite, metagabbro ancestor; BD32, BD48 medium-grade fenites, granitic gneiss ancestor; BD43 high-grade fenite, granitic gneiss ancestor; BD42 high-grade fenite, metagabbro ancestor; BD35, BD55 leucocratic contact fenites. * includes pectolite, tr trace. Results expressed in volume %.

Low-grade fenite

Granite gneiss

Macroscopically, specimen BD58 (Table 1) has a very heterogeneous appearance owing to mm-wide sinuous veinlets and clots of green clinopyroxene and grey wollastonite developed in a leucocratic matrix of variable grain-size. In thin section, the most conspicuous feature is the heteroblastic texture, generated by deformation followed by varying degrees of replacement. Anhedral, fragmented grains of K-feldspar and oligoclase up to 2 mm across are surrounded by a heterogeneous, fine-grained feldspathic matrix, suggesting a mortar texture. Contacts between grains are sutured. The slightly turbid oligoclase grains have displaced twin-lamellae and undulatory extinction. The quartz grains, which make up a minor proportion of the rock, are highly fractured and granulated, and are surrounded by small prisms of aegirine and by fasciculate aggregates of wollastonite. Biotite flakes ($\simeq 1$ vol.%) are partly replaced by a very fine-grained aggregate of feldspar, iron oxides and small prisms of aegirine. Calcite occupies the center of the veinlets or forms xenomorphic grains. The paragenetic relationship between aegirine and wollastonite is ambiguous.

Metagabbro

Specimen BD44 is a homogeneous, undeformed, medium-grained, subophitic black-and-white mottled rock. It contains amphibole and plagioclase, with minor amounts of biotite and magnetite (Table 1). The amphibole, pleochroic olive-green to brown, is magnesian hastingsitic hornblende (Morogan, 1982); it presumably replaced primary pyroxene, and is pre-fenitization. The interstitial plagioclase, An_{25} to An_{36} (microprobe), exhibits a granoblastic-polygonal texture, with almost planar grain-boundaries and triple-point junctions. Magnetite grains are rimmed with titanite. Small, acicular prisms of pale green sodic pyroxene occur with calcite in the andesine and as a "whiskery" rim surrounding all hornblende crystals. Inconspicuous flakes of biotite that predate fenitization (and may indicate early mild K-metasomatism) are also rimmed by sodic pyroxene.

Medium-grade fenite

Granite gneiss

Specimens BD5, BD32 and BD48 are fenitized xenoliths that show a less striking pattern of fractures and veins than in the low-grade equivalent, and a more homogeneous granular texture. In thin section, the higher grade of metasomatism is indicated by more thorough recrystallization and by a simpler assemblage of minerals, largely aegirine-augite and anorthoclase (Table 1). Quartz, totally surrounded by aegirine-augite, occurs in BD32. Relict grains of the original oligoclase show indistinct twin-lamellae and slight turbidity, and are surrounded by a granoblastic aggregate of newly formed alkali feldspar. Large poikiloblastic plates of the latter form by coalescence; included

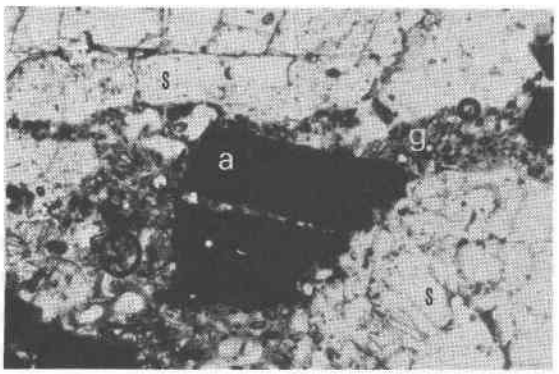

Fig. 2. Metacryst of aegirine-augite (a) in contact with sanidine (s); green glass (g) occurs at the junction of these two minerals in fenitized granite gneiss BD43. The pyroxene is cracked and "intruded" by the melt, which is laden with rounded grains of residual feldspar and pyroxene. Width of field of view 5 mm.

phases are mainly aegirine-augite, titanite and, more rarely, apatite. Aegirine-augite also forms poikiloblastic clusters of stout prisms that enclose aggregates of feldspar. Aegirine-augite replaces wollastonite along grain margins, and in general is associated with titanite.

The specimens of medium-grade fenite are characterized by an almost complete disappearance of the original minerals. Their textures suggest incipient cataclasis, but replacement and recrystallization are dominant. The widespread development of the granoblastic texture and the predominance of the assemblage anorthoclase + aegirine-augite indicate a tendency toward equilibrium under relatively static conditions.

No specimen of fenitized metagabbro showing an analogous stage of development was available for study.

High-grade fenite

Granite gneiss

Specimen BD43 is a medium- to coarse-grained, slightly foliated fenite containing the assemblage sanidine + aegirine-augite + nepheline (Table 1). This assemblage (volume proportions 46:28:5) is considered to have formed at the expense of granite gneiss. The sanidine is Carlsbad-twinned and free of inclusions; it forms elongate crystals or smaller laths that show an alignment. The metacrysts of poikiloblastic pyroxene are strongly embayed, and are surrounded by a film of pale green glass (Fig. 2). The sieve-like aspect of the pyroxene grains may be due to melting of the inclusions, as green glass still occupies some of these holes. The aegirine-augite is partially transformed to hematite. Nepheline grains are euhedral to subhedral. Some grains of titanite appear shattered and display irregular, embayed margins, suggesting that this phase was also involved in the melting reaction. The pale green glass is ubiquitous; it occurs along aegirine-augite–sanidine contacts as well as along fractures and cleavages in feldspar, where it may be associated with wollastonite.

Metagabbro

Specimen BD42 is the highest-grade fenite derived from a metagabbroic ancestor. The medium-grained specimen has an almost homogeneous appearance, and contains the assemblage nepheline + aegirine-augite + sanidine in the proportion 30:51:7 (Table 1). Plagioclase has been completely replaced by nepheline. The aegirine-augite, green to brown, generally forms stout, idioblastic prisms. Its poikilitic texture is due to numerous inclusions of titanite, neph-

Table 2. Representative compositions of clinopyroxene, Oldoinyo Lengai fenites

	BD44		BD58		BD32		BD48	BD47		BD43		BD42		BD35
SiO_2 wt.%	51.47	51.77	52.64	52.25	52.38	52.08	52.67	50.41	51.24	49.77	49.64	51.76	51.52	51.24
Al_2O_3	0.59	0.27	0	0	0	0	0	0.19	0.33	1.13	1.17	0.42	0.70	0.12
TiO_2	0.54	0.74	1.01	2.38	0.47	0.86	1.98	0.38	0.27	0.34	0.53	0.46	0.26	0.46
Cr_2O_3	0.02	0	0.20	0	0	0.16	0.18	0.02	0.12	0.29	0.07	0.17	0.23	0.09
FeO	16.83	17.90	18.88	22.24	18.45	20.48	18.49	17.74	20.30	23.17	22.44	16.29	17.61	24.90
MnO	0.42	0.55	1.66	0.92	0.96	1.02	0.80	0.58	0.82	0.18	0.56	0.76	0.46	0.52
MgO	7.79	7.24	5.69	3.08	6.68	5.52	6.45	6.71	5.72	3.95	3.53	8.04	7.63	2.98
CaO	18.00	14.49	13.02	14.81	15.95	12.85	11.00	17.71	14.89	16.41	15.89	17.65	16.39	13.71
Na_2O	3.09	5.36	6.19	10.41	3.98	5.72	7.05	3.32	4.79	4.27	3.74	3.25	4.18	5.85
K_2O	---	0.11	0.22	0.10	0.14	0.10	0.10	0.10	0.05	0.09	0.22	0.11	0	0.06
total	98.75	98.43	99.50	98.20	99.02	98.79	98.74	98.16	98.35	99.72	97.78	98.91	98.97	99.93
"Quad"	74.9	59.0	52.8	17.8	69.6	56.0	46.4	74.1	63.0	66.8	70.5	75.4	68.3	54.5
"Others"	25.1	41.0	47.2	82.2	30.4	44.0	53.6	25.9	37.0	33.2	29.5	24.6	31.7	45.5
Ac mole %	20.6	37.6	42.7	75.4	27.9	38.3	45.5	21.2	33.7	29.9	27.7	19.5	26.4	36.5
Hd	34.2	24.1	26.4	12.0	34.9	32.1	20.1	40.6	36.4	53.0	45.7	36.3	33.3	47.6
Di	45.2	38.3	30.9	12.6	37.2	29.6	34.4	38.2	29.9	17.1	26.6	44.2	40.3	15.9

Compositions determined by electron-microprobe analysis. In cases where two compositions are provided, the left-hand column shows the composition of the core, and the right-hand column, that of the rim of the same crystal. "Quad" and "Others" are defined in the text. BD44 low-grade fenite, metagabbro ancestor; BD58 low-grade fenite, granitic gneiss ancestor; BD32, BD48 medium-grade fenites, granitic gneiss ancestor; BD47, BD43 high-grade fenites, granitic gneiss ancestor; BD42 high-grade fenite, metagabbro ancestor; BD35 leucocratic contact fenite.

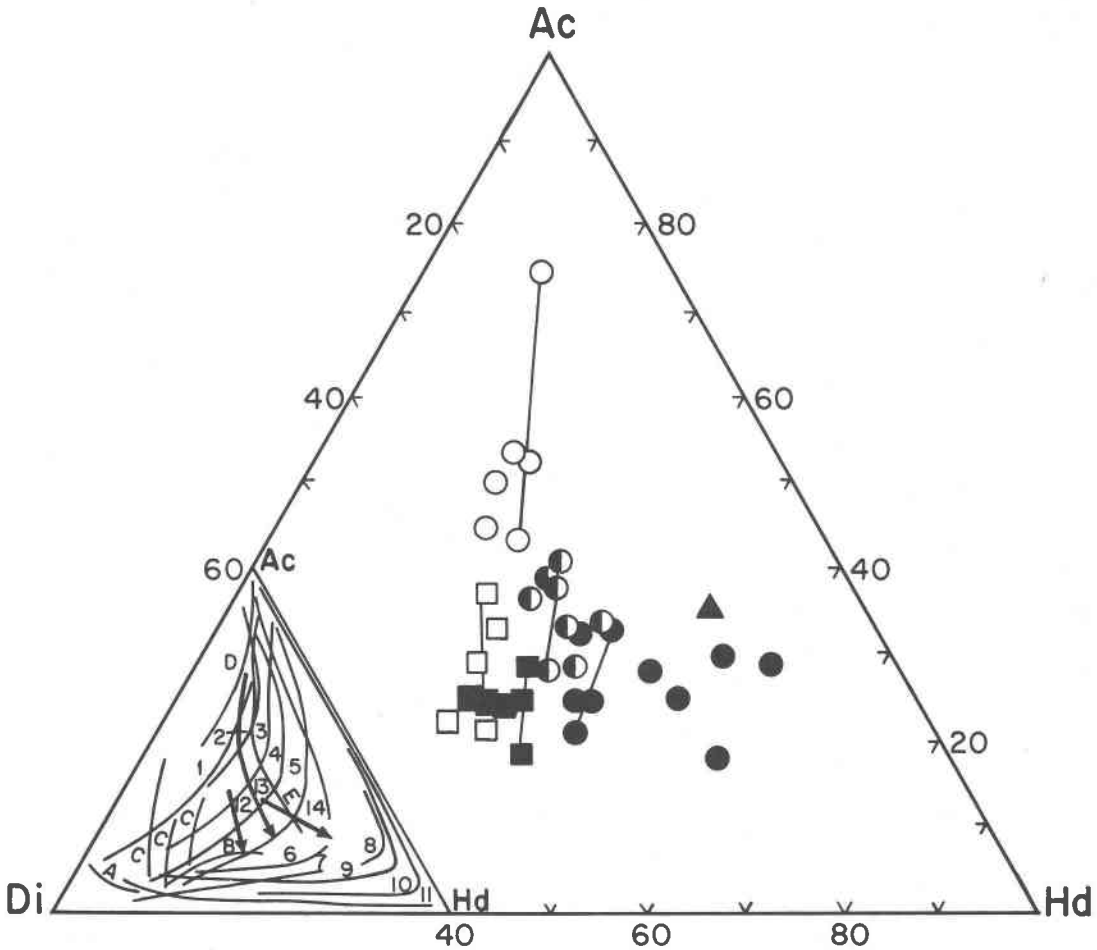

Fig. 3. Compositional variation encountered in the sodic pyroxene, in terms of the principal components acmite (Ac), diopside (Di) and hedenbergite (Hd). Circle: pyroxene in fenites of metagranitic ancestry; square: pyroxene in fenites of metagabbroic ancestry; triangle: pyroxene in contact fenite. Open symbols: low-grade fenite. Half-filled symbols: medium-grade fenite. Filled symbols: high-grade fenite. Zonation trends indicated by solid lines. The inset illustrates the compositional trends of Oldoinyo Lengai metasomatic pyroxene (12, 13, 14, all arrows) in comparison with other trends in alkali pyroxene from undersaturated rocks (1 to 6, 10 and letters) and oversaturated rocks (7 to 9, 11). 1 Auvergne, France (Varet, 1969), 2 Lovozero, U.S.S.R. (Bussen and Sakharov, 1972), 3 Itapirapuã, Brazil (Gomes et al., 1970), 4 Uganda (Tyler and King, 1967), 5 Morotu, Sakhalin (Yagi, 1966), 6 South Qôroq, Greenland (Stephenson, 1972), 7 Japanese alkali basalts (Aoki, 1964), 8 pantellerite trend (Nicholls and Carmichael, 1969), 9 Nandewar volcano, Australia (Abbott, 1969), 10 Ilimaussaq, Greenland (Larsen, 1976), 11 Skaergaard (Brown and Vincent, 1963), A Fen, damkjernite–vibetoite trend, B acmitic hedenbergite trend, C acmitic trend (Mitchell, 1980), D and E Fen, metasomatic pyroxenes (Kresten and Morogan, 1985).

eline and sanidine, probably incorporated during the recrystallization of separate grains of pyroxene into larger crystals. A trace of glass can be found near the pyroxene. Nepheline forms idioblastic, slightly turbid crystals. Sanidine forms interstitial xenomorphic grains and some larger subidioblastic plates; Carlsbad twinning is common. Titanite (6 vol.%) is either idioblastic (characteristic wedge shape) or subidioblastic and poikiloblastic, containing inclusions of sanidine and aegirine-augite.

Contact fenite

Two specimens, BD35 and BD55, are considered examples of what Le Bas (1977) called "contact fenite", rocks that are rather homogeneous and very leucocratic. Both specimens contain more than 85% feldspar (sodic plagioclase + alkali feldspar) in a granular-polygonal array of sutured grains. Both the sodic plagioclase and K-rich feldspar are turbid; the K-feldspar is conspicuously perthitic

Table 3. Microprobe data on feldspars, Oldoinyo Lengai fenites

		BD44	BD32	BD48	BD42		BD43		BD35
SiO_2	wt.%	62.15	67.04	66.62	64.78	63.38	64.35	64.49	68.04
Al_2O_3		23.33	18.08	18.10	17.45	17.22	18.22	17.99	18.40
TiO_2		0.07	-	-	0.15	0.35	0.25	0.39	0.12
Cr_2O_3		0.10	0.20	0.04	-	-	-	-	-
Fe_2O_3		0.19	1.14	0.77	0.49	1.20	0.23	0.35	0.71
MnO		0.02	0.19	-	-	-	-	0.09	-
CaO		4.22	0.16	-	0.06	0.20	-	0.05	0.13
Na_2O		8.62	7.44	8.14	2.88	2.59	3.08	3.24	9.24
K_2O		0.58	4.67	4.83	12.00	12.38	12.21	11.97	1.89
total		99.28	98.92	98.51	97.81	97.32	98.34	98.57	98.53
Composition recalculated in terms of the end-members									
Ab	mol.%	76.1	70.2	72.0	26.6	23.9	27.7	29.1	87.6
Or		2.7	24.4	25.3	71.1	70.5	71.4	69.4	8.9
An		20.6	0.9	-	0.3	1.0	-	0.2	0.7
$KFeSi_3O_8$		0.6	4.5	2.7	1.9	4.6	0.9	1.3	2.9

BD44 low-grade fenite, metagabbro ancestor; BD32, BD48 medium-grade fenites, granitic gneiss ancestor; BD42 high-grade fenite, metagabbro ancestor; BD43 high-grade fenite, granitic gneiss ancestor; BD35 leucocratic contact fenite.

and replaced along its rim by chessboard albite. Thin films of calcite occur locally along the dislocated contacts of some grains. Small subidiomorphic prisms of aegirine-augite and wollastonite (partly altered to pectolite) occur as inclusions in K-feldspar or at grain boundaries. Small grains of melanite are commonly embedded in the albitic rims.

Compositions of minerals

The compositions of the major minerals in the fenitized xenoliths have been determined using an ARL-EMX electron microprobe and a Tracor-Northern NS-880 energy-dispersion system (Queen's University, Kingston, Ontario). The recrystallized alkali feldspars were also analyzed by X-ray diffraction; the indexed patterns, corrected against a spinel internal standard ($a = 8.0833$Å at room temperature), were used to obtain the cell parameters of the feldspars by least-squares refinement (Appleman and Evans, 1973).

Clinopyroxene

Clinopyroxene is the only ferromagnesian phase formed during fenitization. Microprobe traverses were done to evaluate the compositional variations inferred from the variations in optical properties. Representative compositions are provided in Table 2. The amount of Fe^{3+} in sodic pyroxene was estimated using the charge-balance relationship $^{VI}(Al + Fe^{3+} + Cr^{3+} + 2Ti^{4+}) = {}^{IV}Al + {}^{M2}Na$, where the left-hand and right-hand sides represent charge excess and charge deficiency, respectively, relative to components of the pyroxene quadrilateral Di–Hd–Fs–En (Cameron and Papike, 1980).

The clinopyroxene compositions may be considered in terms of a solid solution between quadrilateral components ("Quad") and "Others". Data in Table 2 indicate between 25 and 82% "Others" in the clinopyroxene. The principal non-Quad component clearly is $NaFe^{3+}Si_2O_6$ (Ac); in most instances, the next most prevalent non-Quad component is $Na_2TiR^{2+}Si_4O_{12}$. The compositions are plotted in terms of the main components Di, Hd and Ac in Figure 3. With progressive fenitization, the clinopyroxene in metagranitic material evolves from aegirine (more than 70% Ac) to aegirine-augite (down to approximately 20% Ac). The rim of a zoned grain is richer in Ac. Similarly, Rubie and Gunter (1983) noted an increase in Ac content of the pyroxene away from an intrusive complex causing metasomatism. This most likely reflects, in their opinion, an increasing Na content of the fluid with decreasing temperature. As an alternative, it could also reflect increasing $f(O_2)$ of the fluid. With increasing grade of fenitization, the clinopyroxene becomes less sodic and increasingly depleted in the component Di and enriched in Hd. The pyroxene that coexists with melt plots closest to the Hd apex.

The clinopyroxene in metagabbroic xenoliths covers a less extensive compositional range, between $Di_{38}Hd_{24}Ac_{38}$ and $Di_{44}Hd_{36}Ac_{20}$, and displays a higher proportion of Di, reflecting the more magnesian original bulk-composition. It shows a progressive enrichment in Ac from high to low grade and from core to rim. The Jd component attains a maximum value of 4%.

The concentration of titanium attains a maximum of 0.07 atoms per formula unit (a.f.u.) in low-grade fenites (Table 2). The concentration drops to below 0.02 a.f.u. in almost all analyzed grains in the high-grade fenites. Aluminum is present in clinopyroxene from the low-grade metagabbroic sample (0.07 a.f.u.), but is absent from that in the low-grade metagranitic material. The pyroxene that coexists with melt has the highest concentration of Al recorded in high-grade rocks, 0.06 a.f.u.

The inset in Figure 3 allows a comparison of compositional trends at Oldoinyo Lengai (numbered 12, 13 and 14) with those for other suites. Trends 1 to 6 pertain to clinopyroxene from SiO_2-undersaturated rocks, and trends 7 to 11 pertain to clinopyroxene from SiO_2-oversaturated suites. Trends A, B and C depict magmatic pyroxene from the Fen alkaline carbonatitic complex, whereas D and E represent compositional trends of metasomatic pyroxene in the related fenites. Although the Oldoinyo Lengai compositions plot in the field of clinopyroxene from SiO_2-undersaturated suites (whose trends are governed by fractional crystallization), the trends defined by metasomatic clinopyroxene are distinctive. Trends 12 and 13 parallel E, relevant to fenitization of metagranitic material by emanations from carbonatitic magma at Fen (Kresten and Morogan, 1985). Whereas with fractional crystallization, Mg decreases continuously with increasing Fe^{2+} and, ultimately, Na^+ (Fe^{3+}), trends of progressive fenitization indicate a steadily decreasing Na^+ (Fe^{3+}) and increasing Fe^{2+} as Mg decreases.

Feldspar

Selected microprobe data are reported in Table 3 and plotted in the diagram An–Ab–Or (Fig. 4). The only feldspar present in the low-grade metagabbroic fenite is plagioclase in the andesine–oligoclase range. Except for two compositions in the oligoclase range from the leucocratic con-

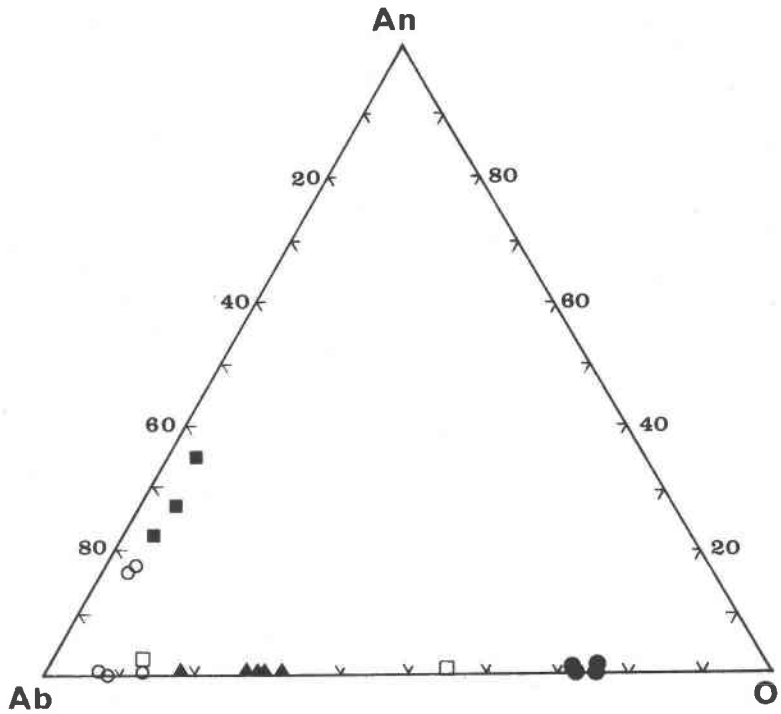

Fig. 4. Composition of relict and newly formed feldspars in the fenites, as determined by electron microprobe. Plot is in molar proportions. Open square: feldspar in low-grade fenite of metagranitic ancestry. Filled square: feldspar in low-grade fenite of metagabbroic ancestry. Filled triangle: feldspar in medium-grade fenite, metagranitic ancestry. Filled circle: feldspar in high-grade fenite. Open circle: feldspar in contact fenite. Note that the alkali feldspar compositions closely approach the binary system Ab–Or.

tact fenite, all other feldspar compositions plot in the system Ab–Or. The sodic alkali feldspar commonly shows cross-hatched domains in thin section, indicating that it formed as a monoclinic structure that inverted to triclinic symmetry upon cooling. It is thus referred to as anorthoclase. The composition of the anorthoclase from low- and medium-grade fenites and from one specimen of contact fenite lies between Or_8 and Or_{32}, in fairly good agreement with the compositions derived from X-ray-diffraction data (see below). Sanidine (Or_{71}) characterizes the specimens of high-grade fenite. At first glance, the compositions shown in Figure 4 do not seem consistent with a high temperature

Table 4. Unit-cell parameters of feldspars, Oldoinyo Lengai fenites

	a	b	c	α	β	γ	V	α^*	β^*	γ^*	$\Delta 2\theta$	#
BD58	8.2403	12.9219	7.1458	91.189	116.240	90.087	681.84	87.516	63.736	88.823	0.009	19
	0.0010	0.0013	0.0012	0.013	0.009	0.009	0.11	0.011	0.009	0.009		
	8.6162	12.9990	7.1857	90	115.977	90	723.51	90	64.977	90	0.018	18
	0.0020	0.0037	0.0020		0.025		0.25		0.025			
BD5	8.2433	12.9369	7.1437	92.318	116.420	90.191	681.50	87.317	63.548	88.634	0.019	31
	0.0015	0.0059	0.0011	0.030	0.014	0.027	0.28	0.026	0.014	0.024		
BD32	8.2766	12.9603	7.1556	91.500	116.332	90.209	687.59	88.223	63.652	89.024	0.014	56
	0.0008	0.0016	0.0007	0.013	0.009	0.013	0.10	0.014	0.009	0.015		
BD48	8.2738	12.9601	7.1511	91.622	116.347	90.176	686.77	88.102	63.636	89.000	0.010	38
	0.0006	0.0015	0.0006	0.013	0.007	0.009	0.09	0.013	0.007	0.009		
BD42	8.6028	13.0193	7.1727	90	116.019	90	721.93	90	63.981	90	0.027	51
	0.0016	0.0028	0.0014		0.016		0.18		0.016			
BD43	8.6027	13.0240	7.1785	90	115.992	90	722.94	90	64.008	90	0.022	53
	0.0011	0.0025	0.0010		0.012		0.14		0.012			
BD55	8.2116	12.9115	7.1440	92.626	116.595	90.157	676.35	86.983	63.367	88.508	0.021	36
	0.0022	0.0022	0.0014	0.018	0.015	0.019	0.17	0.017	0.014	0.019		

BD58 low-grade fenite, granitic gneiss ancestor; BD5, BD32, BD48 medium-grade fenites, granitic gneiss ancestor; BD42 high-grade fenite, metagabbro ancestor; BD43 high-grade fenite, granitic gneiss ancestor; BD55 leucocratic contact fenite. Units: a, b, c and $\Delta 2\theta$ (the mean standard error associated with the raw data) in Å, the unit-cell volume in $Å^3$, and α, β, γ, α^*, β^*, γ^* in degrees. # represents the number of indexed reflections used in the refinement, carried out with the program of Appleman & Evans (1973).

Table 5. Indicators of composition and structure of feldspars

	$N_{Or}(V)$	$\Delta(bc)$	$\Delta(\alpha^*\gamma^*)$	t_1O	Or(*)
BD58	0.210	0.597(8)	0.030(5)	0.313	0.461
	1.019	0.666(16)	0	0.333	0.971
BD5	0.205	0.547(16)	-0.010(12)	0.274	0.425
BD32	0.292	0.565(6)	-0.040(8)	0.283	0.609
BD48	0.280	0.537(5)	-0.023(5)	0.269	0.578
BD42	0.971	0.527(12)	0	0.264	0.961
BD43	1.001	0.553(9)	0	0.278	1.006
BD55	0.112	0.610(10)	0.008(9)	0.309	0.291

The indicators are calculated from cell-dimension data (Table 4). The specimens are identified in Table 4. Definitions: $N_{Or}(V)$ mole fraction of Or based on unit-cell volume; $\Delta(bc) = t_1O + t_1m$; $\Delta(\alpha^*\gamma^*) = t_1O - t_1m$; t_1O and t_1m represent the Al occupancy of the T_1O and T_1m positions, respectively. In monoclinic feldspars, $t_1O = t_1m$ and $\Delta(\alpha^*\gamma^*) = 0$. Or(*): mole fraction of Or based on co-ordinates in a plot of b^* *versus* α^* (Blasi 1977). In an alkali feldspar free of impurities and of strain affecting the a dimension, Or(*) should equal the mole fraction of Or calculated on the basis of unit-cell volume.

of equilibration, as the compositions are close to being truly binary. However, a greater amount of the An component in sanidine could only be expected where that sanidine *coexists* with plagioclase (cf. Parsons and Brown, 1984). The fact that these sanidine and anorthoclase compositions are low in calcium is consistent with the proposal that they were deposited from a fluid phase rich in alkalis but depleted in calcium, and thus are not in equilibrium with a coexisting plagioclase. Such examples of Ca-poor, high-temperature (Na,K)-feldspars are exceedingly scarce in nature, although they can readily be synthesized. Lehtinen and Sahama (1981) reported on similar unexsolved, disordered (Na,K)-feldspars in partially fused granite xenoliths transported to the surface by melilite nephelinite lava in the volcano Nyiragongo, in eastern Zaire.

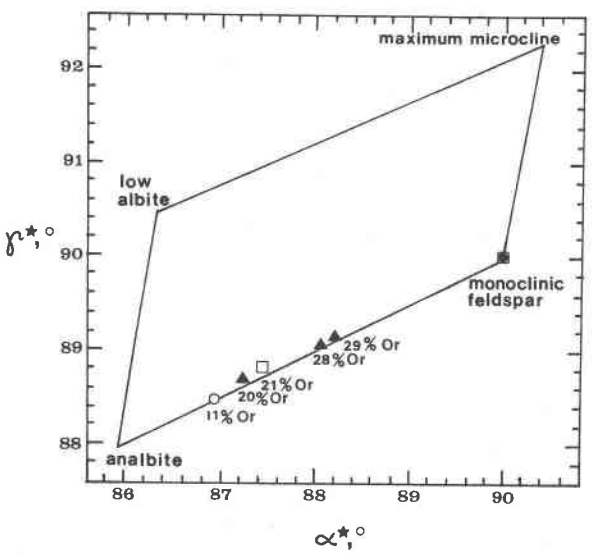

Fig. 5. Plot of α^* versus γ^* for the alkali feldspar compositions that occur in the fenitized xenoliths. Open square: feldspar from low-grade fenite. Filled triangle: feldspar from medium-grade fenite. Filled circle: feldspar from high-grade fenite. Open circle: feldspar from contact fenite. Or content (in mol. %) is given for anorthoclase data-points. Symbols are larger than the standard error in α^* and γ^*.

The near-absence of calcium in the alkali feldspar means that the results of a detailed X-ray-diffraction analysis can be interpreted straightforwardly by reference to the binary system. Cell dimensions, refined by least squares using carefully indexed diffraction-maxima, are reported in Table 4; values of the structural indicators and estimates of tetrahedral site-occupancies are presented in Table 5.

A plot of the reciprocal lattice angles α^* versus γ^* (Fig. 5) shows that the feldspar samples, though variable in composition, are all highly disordered, as they are strung out along the sideline linking analbite and monoclinic K-feldspar (all compositions in which $\alpha^* = \gamma^* = 90°$ reduce to a point in this plot). The cell dimensions b and c (Fig. 6, plot contoured for a) indicate that not all samples are equally disordered. The sample of low-grade metagranitic fenite (BD58) contains two feldspars, one monoclinic and K-rich, the other anorthoclase. Both feldspars display a balanced distribution of Al in the T_1O and T_1m sites (Table 5), i.e., the Na-rich feldspar, though triclinic, is topochemically monoclinic. The two feldspars are not related by unmixing, as the anorthoclase forms fine recrystallized grains with sutured, intricate boundaries between the larger cores of sanidine or in bands diagonally crossing the sanidine cores. We contend that the deformation history of the original feldspar grains controls the present distribution of the two feldspars; the fractured crystals were permeated rapidly by the alkali-rich fluid, leading to deposition of a disordered (monoclinic) Na-rich feldspar. Feldspars in the binary system $NaAlSi_3O_8$–$KAlSi_3O_8$ are known to equilibrate rapidly in terms of composition in the presence of an alkaline fluid phase (Martin, 1973). However, these two feldspars cannot be considered to be in compositional equilibrium.

The two feldspars in BD58 happen to be the most ordered of the group. The values of t_1O, the proportion of Al in the T_1O position, are 0.31 and 0.33 for the sodic and potassic phases, respectively (Table 5); t_1O is 0.25 in a completely disordered feldspar and 1 in its fully ordered equivalent, so that both feldspars are still relatively disordered. Their progress toward a more ordered assemblage could be explained in terms of a lower temperature of metasomatism than was the case for higher-grade rocks. The degree of order attained resembles that in K-bearing sodium-rich feldspars synthesized in the range 650–700°C in experiments held at 2.5 kbar for ten days (Martin, 1974). As in the case studied by Lehtinen and Sahama (1981), two factors point to a rapid quench of the xenoliths: (1) the disordered nature of the feldspars, especially those that are enriched in Na in view of their greater reactivity (Martin, 1974), and (2) the absence of exsolution lamellae in the newly formed feldspars. The temperature of the xenoliths dropped from the range of 700 to 800°C, presumably by entrainment in a rising plume of lava.

The presence of the cross-hatch pattern in the relatively

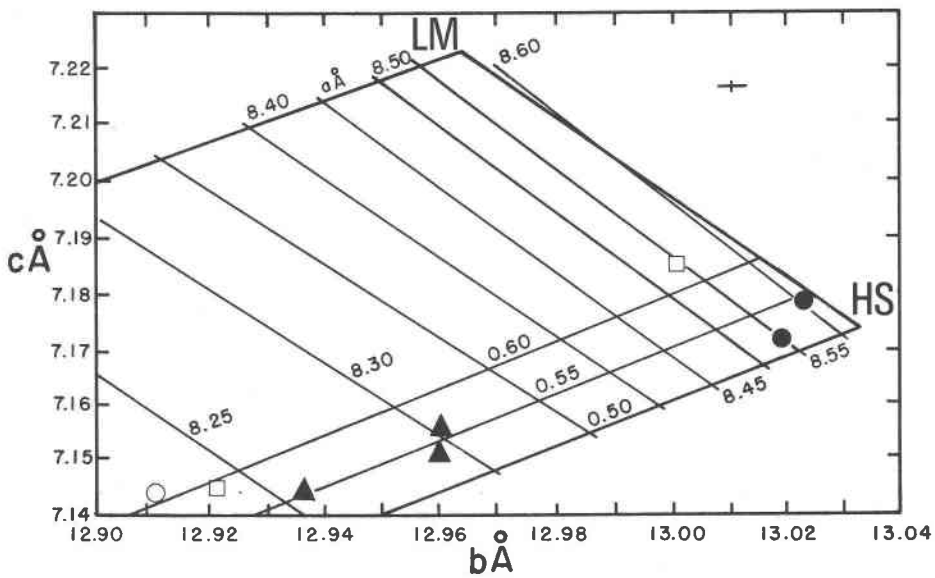

Fig. 6. Cell dimensions of alkali feldspar samples investigated, shown on the *a*-contoured $b - c$ quadrilateral of Wright and Stewart (1974). Symbols are as in Figure 5. A comparison of the predicted *a* dimension (from the contours) with the value obtained by cell refinement (Table 4) shows that all these samples contain an anomalous alkali feldspar, though apparently not because of exsolution-induced strain. The average standard error associated with *b* and *c* is shown in the upper right corner. HS refers to high sanidine, disordered $KAlSi_3O_8$; LM refers to the ordered equivalent. The contours labeled 0.50, 0.55, 0.60 refer to the sum of Al in the T_1 sites (0.50 in a completely disordered alkali feldspar).

sodic anorthoclase in fenite BD55 (Or_{11}, as inferred from unit-cell volume: Table 5) implies that this feldspar crystallized as a monoclinic phase. Relevant data on synthetic feldspars on the join Ab–Or indicate that inversion of monoclinic Or_{11} to a triclinic phase occurs close to 760°C (Kroll, 1971). This sets a minimum temperature of formation that agrees with the deduction based on degree of order attained.

Table 6. Composition of nepheline in high-grade fenite

		Fenite BD43			Fenite BD42	
SiO_2	wt.%	44.55	44.25	43.70	43.84	42.40
Al_2O_3		30.53	31.79	31.10	31.42	32.46
TiO_2		-	-	-	-	0.08
Cr_2O_3		0.08	-	-	-	0.05
FeO		1.70	0.84	1.70	1.04	1.81
MnO		-	-	-	0.02	0.03
CaO		0.09	-	0.09	0.06	0.11
Na_2O		15.50	14.56	14.32	14.80	14.55
K_2O		5.14	6.20	6.34	6.83	7.56
total		97.59	97.64	97.25	98.01	99.05
Recalculation in terms of nepheline + kalsilite + quartz						
Ne	mol.%	74.41	71.45	71.04	70.79	71.19
Kls		16.21	19.99	20.67	21.50	24.35
Qtz		9.38	8.50	8.28	7.70	4.45
Composition of the coexisting potassium-rich alkali feldspar						
Ab	mol.%	26.87	24.85	-	20.86	22.31
Or		73.03	75.14	-	78.12	77.38
An		0.10	0	-	1.00	0.30

Microprobe data. BD43 granitic gneiss ancestor; BD42 metagabbro ancestor.

The two specimens of high-grade fenite examined contain a very potassium-rich sanidine. A trend away from the sodium end-member resembles the trend noted in the coexisting pyroxene (buildup in the component Hd), and may also be due to the partition of Na into coexisting phases (nepheline, melt, fluid) at the highest grade. The degree of Al-Si order attained in these specimens (t_1O 0.26, 0.28) is consistent with a temperature of crystallization close to 900°C (Stewart and Wright, 1974, Fig. 6). The absence of microcline, which is the K-feldspar typical of fenites, is consistent with the interaction of basement rocks with an alkaline fluid above 500°C, considered the upper limit of its field of stability (Bernotat and Morteani, 1982).

Nepheline

Nepheline is restricted to high-grade fenites, and is found in greatest abundance (>30% by volume) in sanidine-bearing nepheline aegirine-augite fenite BD42. The composition of nepheline and of the coexisting sanidine is given in Table 6. The departure of the composition from the binary join Ne–Ks may be used as an approximate indication of temperature of equilibration with alkali feldspar. The relevant part of the system quartz–nepheline–kalsilite is shown in Figure 7, with the limits of solid solution drawn for 500, 700, 775 and 1068°C, as determined experimentally at low pressures by Hamilton (1961). The composition of the nepheline is enriched in Si relative to that of nepheline expected in plutonic rocks, and falls in the field of nepheline typically found in effusive rocks, above the 775°C iso-

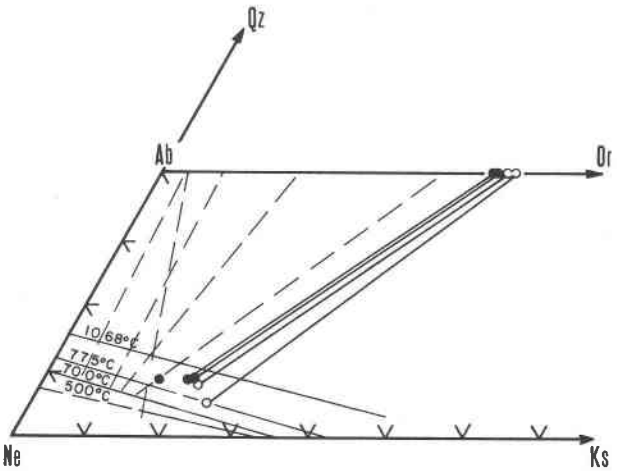

Fig. 7. The composition of coexisting nepheline and K-rich feldspar in high-grade fenite plotted in the system quartz–nepheline–kalsilite. Limits of solid solution in nepheline at 500° (2 kbar), 700° and 775°C (1 kbar) from Hamilton (1961). Also shown is the limit determined at 1 atmosphere (1068°C). Experimentally determined tie-lines are shown as dashed lines. Filled circle: nepheline + K-feldspar pair from nepheline-bearing sanidine aegirine-augite fenite (BD43) formed from metagranitic ancestor. Open circle: nepheline + K-feldspar pair from sanidine-bearing nepheline aegirine-augite fenite (BD42) formed from metagabbroic ancestor.

therm. The trend of the nepheline–sanidine tie-line is consistent with experimentally determined tie-lines for pairs equilibrated above 700°C.

The temperature of last equilibration of the pair nepheline–sanidine in the fenite xenoliths may be estimated using the geothermometer of Perchuk and Ryabchikov (1968) and Powell and Powell (1977). The calculated temperature, 850°C, is in fairly good agreement with the inference made from Figure 7. The low concentration of calcium in the nepheline ($\simeq$0.10 wt.% CaO) and coexisting sanidine means that the geothermometer should give reliable results, though a correction would have to be made for the small proportion of Fe^{3+} substituting for Al. The relatively high departure from the binary join Ne–Ks was presumably preserved as a result of a rapid quench of the xenoliths, which prevented the type of subsolidus adjustment in the Si/Al ratio expected in plutonic nepheline in contact with a K-rich alkali feldspar.

Composition of the glass

Small amounts of glass have been recognized in xenoliths of high-grade fenite. Partial melting is most widespread in BD43, a nepheline-bearing sanidine aegirine-augite fenite. The rock contains films of greenish glass located near embayed and sieve-like grains of clinopyroxene (Fig. 2). The composition of the glass in the largest patches was determined using the electron microprobe (energy dispersion) with a low beam-current (6 μA) to minimize the loss of light elements by volatilization (Table 7). In general, the sum of the oxides falls short of 100% by 5 to 10%. This shortfall probably represents volatile components of the glass. The presence of Cl and S has been confirmed by qualitative energy-dispersion analyses.

Two distinct varieties of glass occur in BD43: (1) a SiO_2-undersaturated peralkaline glass, and (2) a SiO_2-oversaturated peraluminous glass. These are conveniently shown in terms of the molar proportions of SiO_2, Al_2O_3 and $(Na_2O + K_2O)$ (Fig. 8).

SiO_2-undersaturated peralkaline glass

The presence of Ne, Ac and Ns in the norm and the high value of the agpaitic index [(Na + K)/Al] of 1.65 confirm the SiO_2-undersaturated peralkaline nature of this type of glass, which occurs at the boundaries of pyroxene and sanidine grains. The glass is characterized by a molar ratio Na/(Na + K) of 0.56. Its bulk composition could be explained by the partial melting of the assemblage aegirine-augite + nepheline + sanidine. In order to test this hypothesis, we used the least-squares mineral-distribution program of Wright and Doherty (1970). Of several combinations of minerals used, we found that the above assemblage, in the approximate proportion 40:30:30, best accounts for the composition of the Ne-normative peralkaline melt, as measured by the smallest difference between measured and calculated compositions of the glass (discrepancy in total oxides 7 wt.%). The calculated content of the alkalis, and especially of K, is lower than the measured concentration (difference > 2%), which might reflect the in-

Table 7. Compositions of partial melts (glass) developed in BD43

		1	2	3	4	5
SiO_2	wt.%	47.98	49.03	59.77	55.62	55.80
TiO_2		1.48	0.81	1.03	1.36	0.11
Al_2O_3		11.09	13.18	13.40	12.26	11.90
Fe_2O_3	*	7.09	5.54	3.58	4.10	3.00
FeO		3.40	3.40	3.50	3.37	4.40
MnO		0.05	0.23	0.61	0.43	0.00
MgO		0.43	0.16	0.00	0.00	1.62
CaO		4.83	3.25	4.84	5.22	10.28
Na_2O		6.33	7.59	1.41	1.14	2.43
K_2O		7.31	9.16	6.97	4.52	9.00
P_2O_5		na	na	na	na	1.45
total		89.99	92.35	95.11	88.02	99.99
Normative constituents (weight basis) summed to 100%						
Lc		14.54	30.34			1.75
Ns		3.60	7.36			
Or		29.47	19.91	31.90	30.35	50.96
Ab				12.54	10.96	
Qtz				17.14	25.27	
An				10.15	17.03	
Ne		9.85	9.85			6.02
Di		10.71	11.79	5.74	2.90	23.37
Wo		5.93	1.71	3.62	3.82	5.84
Ac		22.79	17.36			8.33
Il		3.12	1.67	2.06	2.93	0.21
Mt				5.46	6.75	0.17
Ap						3.37
A.I.		1.65	1.69	0.73	0.55	1.15
Na/(Na + K)		0.57	0.56	0.23	0.27	0.29

Compositions of glass determined by electron microprobe. Columns 1, 2: SiO_2-undersaturated peralkaline glass; columns 3, 4: SiO_2-oversaturated peraluminous glass; column 5: bulk composition of fenite BD43, determined by X-ray fluorescence. * Ratio of ferrous iron to ferric iron assumed to be that in the coexisting clinopyroxene. na not analyzed, A.I. agpaitic index [(Na + K)/Al].

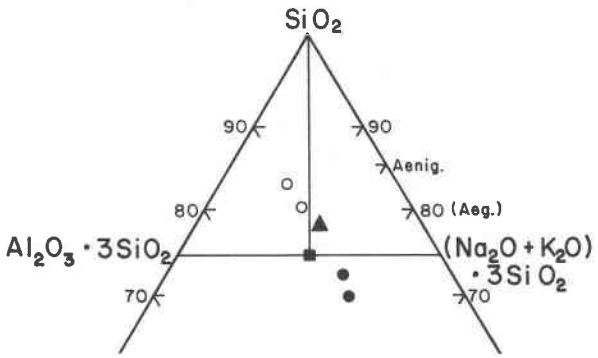

Fig. 8. The composition of glass found in partially melted fenite BD43, in terms of the system SiO_2–Al_2O_3–($Na_2O + K_2O$). Square: stoichiometric feldspar. Triangle: bulk composition of fenite BD43. Open circle: SiO_2-oversaturated glass. Filled circle: SiO_2-undersaturated glass.

congruent melting of the acmite component of the clinopyroxene and the net addition of potassium to the system at the time melting occurred.

SiO_2-oversaturated peraluminous glass

The slightly SiO_2-oversaturated glass typically occurs along fractures within feldspar and, locally, is intimately associated with wollastonite. The glass is quartz-normative, peraluminous (agpaitic index 0.63) and has a low Na/(Na + K) ratio (0.25; Fig. 8). These general features suggest that sanidine could be a possible candidate for a partial-melting reaction. However, the high Ca and Fe contents imply the contribution of another phase. The best candidate is the assemblage sanidine + hedenbergite (component in the pyroxene) in the proportion 74:26 (discrepancy in total oxides: 6.5 wt.%). The higher calculated alkali content of the melt, compared to that measured in the glass (discrepancy especially in K) may indicate loss of alkali into a vapor phase present during the melting event; the strongly aluminous bulk-composition may also be due to the preferential loss of alkalis.

The occurrence of two widely different compositions of glass in one specimen may be due to disequilibrium melting. Blocks of metasomatized basement rocks were suddenly picked up by lava and heated rapidly above the solidus of the fenitic assemblage. Melting could be expected to begin at several places depending on the specific combination of reactants, leading to different compositions of melts. The suddenness of the eruption would have allowed no time for the disparate compositions to homogenize. This proposal is consistent with the lack of re-equilibration of feldspar and nepheline and of devitrification, which could have been expected if cooling had occurred more slowly. If the blocks of fenite became rheomorphic due to soaking in the natrocarbonatite magma that made Oldoinyo Lengai famous, however, it would seem likely that the magma's temperature was somewhat higher than the temperature of the anhydrous liquidus, 655°C at 1 kbar, determined by Cooper et al. (1975).

Table 8. Bulk composition of fenites, Oldoinyo Lengai

		BD44	BD58	BD32	BD48	BD42	BD43
SiO_2	wt.%	46.16	63.58	59.12	55.75	46.12	55.80
TiO_2		0.41	0.11	0.05	0.06	0.53	0.11
Al_2O_3		14.44	11.06	9.88	9.30	12.34	11.90
Fe_2O_3		5.51	3.40	3.64	5.00	5.74	3.00
FeO		3.00	1.14	2.70	2.34	5.76	4.40
MgO		10.33	2.48	4.13	6.49	5.92	1.62
CaO		13.02	10.47	12.73	12.33	12.16	10.28
Na_2O		3.87	3.20	5.04	4.75	5.44	2.43
K_2O		1.39	4.23	2.29	2.09	3.47	9.00
P_2O_5		0.44	0.32	0.44	0.86	1.45	1.45
total		98.57	99.99	100.02	98.97	98.93	99.99
Composition expressed in cations per 100 oxygen anions							
Si		28.47	36.77	35.00	33.53	29.01	33.93
Ti		0.19	0.05	0.02	0.03	0.25	0.05
Al		10.50	7.47	6.89	6.59	9.18	8.53
Fe^{3+}		2.56	1.48	1.50	2.26	2.72	1.37
Fe^{2+}		1.55	0.55	1.34	1.18	3.04	2.24
Mg		9.50	2.14	3.64	5.82	5.56	1.47
Ca		8.61	6.49	8.07	7.94	8.82	6.70
Na		4.63	3.59	5.78	5.54	6.65	2.86
K		1.10	3.12	1.73	1.60	2.79	6.98
P		0.23	0.16	0.22	0.44	0.77	0.74
Agpaitic index		0.55	0.90	1.09	1.13	1.03	1.15

Composition determined by X-ray fluorescence. BD44 low-grade fenite, metagabbro ancestor; BD58 low-grade fenite, granitic gneiss ancestor; BD32, BD48 medium-grade fenites, granitic gneiss ancestor; BD42 high-grade fenite, metagabbro ancestor; BD43 high-grade fenite, granitic gneiss ancestor.

Bulk composition of the rocks

The bulk compositions of six specimens, determined by X-ray fluorescence, are listed in Table 8; results are recalculated to a standard cell of 100 oxygen atoms. The two specimens attributed a metagabbroic origin clearly are different from the four considered to have formed by fenitization of granite. All six, however, share a generally high concentration of calcium. The variation in Si illustrates the two different ancestors of the fenites and their different behavior with progressive fenitization; the four formed from a granitic ancestor are progressively depleted in Si, whereas Fe, Ti and P were added. The fenites resulting from an initially gabbroic composition display slightly increased Si and a depletion in Al and Mg. The data are consistent with a tendency to convergence in the fenitic product, whatever its parentage, to a peralkaline mafic, relatively sodic syenite composition. Much more information would be required to document these trends properly.

Figure 9 illustrates the composition of the six samples in terms of their proportions of normative nepheline, kalsilite and quartz. The diagram, taken from Woolley (1969), shows that there are two evolutionary trends followed in the basement xenoliths at Oldoinyo Lengai. The metagranitic compositions are feldspathized, then K-metasomatized, becoming ultrapotassic fenites at the highest grades. The fenites formed at the expense of gabbro "arrive" in the system Ne–Ks–Qtz via a nephelinitization reaction, possibly of the type (simplified) $CaAl_2Si_2O_8$ +

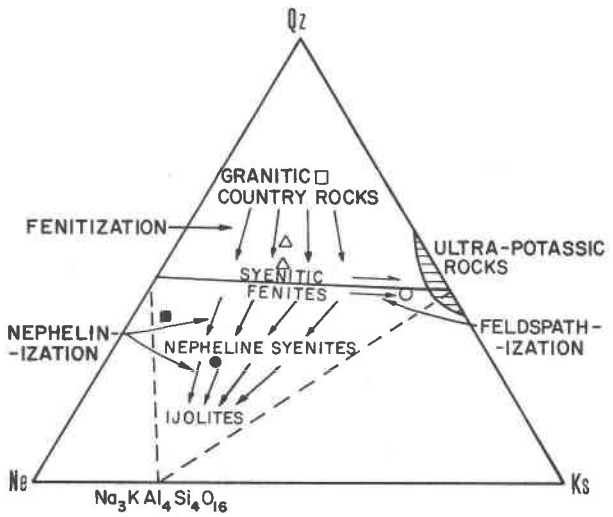

Fig. 9. Plot of compositions of fenite xenoliths in the system nepheline–kalsilite–quartz. Open symbols: fenites formed by metasomatism of metagranitic ancestor. Closed symbols: fenites formed by metasomatism of metagabbroic ancestor. Square: low-grade fenite. Triangle: medium-grade fenite. Circle: high-grade fenite. The arrows indicate the principal compositional changes that occur during alkali metasomatism (Woolley, 1969). In the case of the Oldoinyo Lengai suite, we contend that the silica-undersaturated fenites entered this system by the efficient conversion of plagioclase to nepheline rather than by desilication of feldspathic fenite (syenitic fenite), as indicated by Woolley's arrows.

$(Na,K)_2CO_3 = 2(Na,K)AlSiO_4 + CaCO_3$ (Cermignani and Anderson, 1983).

Discussion

Investigators of the phenomenon of fenitization have been aware of the possibility that a melt phase could be expected at an advanced stage of metasomatism in those parts of the system closest to the heat source. This inference was based mainly on field and textural evidence and on the bulk composition of the mobilized fraction, found in dikes and other cross-cutting bodies. However, details of the observed feldspar mineralogy and the absence of phenocrystic leucite, a phase expected on the liquidus of potassium-rich bulk compositions at low confining pressures, led Sutherland (1965) to hesitate about endorsing the actual melting of fenites and to conclude that "the nature of the process of mobilization is not sufficiently understood".

The importance of the Oldoinyo Lengai xenoliths lies in the documentation of (1) the mineral assemblages present at high temperatures, and (2) the inception of melting, albeit of a disequilibrium type, in the highest-grade fenites. The mineral assemblages present suggest a temperature of melting close to 800°C. Temperatures of melting inferred from the dry system Na_2O–Al_2O_3–Fe_2O_3–SiO_2 (Bailey and Schairer, 1966) are higher than this, but addition of the other components would lower the temperature of melting. Nolan (1966) found solidus temperatures close to 700°C in the related system $NaAlSi_3O_8$–$NaAlSiO_4$–$NaFeSi_2O_6$–$CaMgSi_2O_6$ in the presence of water at a low confining pressure (1 kbar). Information on a directly relevant synthetic system is unfortunately not yet available.

Fusion probably was provoked by the sudden heating or decompression of the hot fenitized xenoliths; these had equilibrated to a somewhat lower temperature before being picked up by the invading carbonatitic magma. Most likely, this event was of short duration, leading to the formation of films of melt at grain boundaries, and to the freezing of the rheomorphic assemblage before equilibration could occur on a hand-specimen scale, possibly as a result of rapid ascent toward the surface.

The limited compositional data on the glass encountered may be plotted on variation diagrams versus wt.% SiO_2 together with the entire range of lava compositions from Oldoinyo Lengai, as reported by Donaldson and Dawson (1978). The melts formed in situ in fenitized granite BD43 parallel the trend phonolite–trachyte encountered, but the lower Al and, in the more siliceous melt, higher Ca and lower Na contents, suggest a greater similarity with feldspar ijolite and alkali syenite compositions. The point being made here is not that the observed compositions of melt match those of known eruptive silicate rocks in the region, but that the process of anatexis of fenitized lower crust could be responsible for the unusual juxtaposition, in the Oldoinyo Lengai area, of the alkali basalt-olivine nephelinite and nephelinite–carbonatite associations, should the process be allowed to progress beyond a small scale.

There have been two principal proposals concerning the genetic relation between the silicate and alkali carbonatite magmas: (1) extreme fractional crystallization of an appropriate silicate (e.g., ijolitic) magma, yielding as residuum the alkali carbonatite (Heinrich, 1966; Watkinson and Wyllie, 1971), and (2) liquid immiscibility relationship between a carbonated silicate and alkali carbonatite magmas (Cooper et al., 1975; Le Bas, 1977; Hamilton et al., 1979; Donaldson and Dawson, 1978). Donaldson and Dawson proposed, for Oldoinyo Lengai, a carbonated phonolitic or nephelinitic liquid as suitable parental material. They considered the parent liquid significantly less mafic than the carbonated melanephelinitic parent proposed by Le Bas (1977). We propose yet a different scenario to explain this enigmatic association.

In the Tanzanian sector of the Gregory Rift, site of Oldoinyo Lengai, the volcanos active before a Pleistocene episode of rifting produced quiescent flows of alkali basalt and olivine-rich nephelinite lavas. Regional swelling of the crust had occurred, and presumably had led to partial fusion in the uppermost mantle upon its decompression. We contend that during the formation of the mantle-derived alkali basaltic melt, a volatile phase rich in water and carbon dioxide and bearing alkalis invaded the lower crust along the axis of the zone of swelling and led to its fenitization on a regional scale. Typical material of the lower and middle crust, such as mafic granulite (Dawson,

1977) and amphibolitized gabbro and granitic gneiss, could be transformed into nepheline–alkali feldspar–clinopyroxene–carbonate fenitic assemblages that could form a suitable fertile parent for the generation, as a result of anatexis, of *conjugate* phonolitic to trachytic and carbonatitic magmas erupted explosively after the episode of Pleistocene rifting in the area. In addition to explaining the secular change in lava composition, this hypothesis also accounts for the juvenile nature of the carbonatite [isotopic data on carbon and oxygen of Vinogradov et al. (1971), Denaeyer (1970) and O'Neil and Hay (1973)] and the apparently comagmatic nature of the nephelinite, phonolite and alkali carbonatite (strontium isotope data of Bell et al., 1973).

The episode of regional fenitization of lower crustal rocks, leading to plagioclase-free rocks containing instead nepheline + carbonate (cf. von Eckermann, 1948), would thus be a critical first step in order to promote the formation of an alkali-rich carbonatitic liquid and phonolitic to trachytic magma. Cermignani and Anderson (1983) found that the nephelinization of plagioclase is favored where carbonate is the main anionic complex (as opposed to chloride) because the carbonates are more strongly dissociated than the analogous chlorides. The lower crust located directly above degassing mantle should probably be considered the optimum setting for the efficient conversion of plagioclase to nepheline because of the high proportion of CO_2 in the fluid medium. Anatectic reactions involving strongly fenitized lower crustal material, as documented in this paper, could be responsible for the juxtaposition of phonolitic to trachytic and alkali carbonatitic melts with mantle-derived nephelinitic magmas at Oldoinyo Lengai.

Acknowledgments

We are grateful to Dr. J. Barry Dawson for his gift of the specimens, continued encouragement and a great deal of patience. We thank Professor D. M. Francis and Messrs. Teodor Morogan and Richard Yates for their contributions to this study, and Ms. Vicki Trimarchi for her valuable assistance in the final stage of preparation of the manuscript. The microprobe data reported here were obtained at Queen's University, Kingston, Ontario; we acknowledge the assistance and hospitality of Professor P. Roeder and Mr. D. Kempson. Drs. A. R. Woolley, J. A. Speer and an anonymous reviewer commented on an earlier version of the manuscript. Research costs were covered by a Natural Sciences and Engineering Research Council grant (A7721) to Robert F. Martin.

References

Abbott, M. J. (1969) Petrology of the Nandewar volcano, N.S.W., Australia. Contributions to Mineralogy and Petrology, 20, 115–134.

Aoki, K. (1964) Clinopyroxenes from alkaline rocks of Japan. American Mineralogist, 49, 1199–1223.

Appleman, D. E. and Evans, H. T., Jr. (1973) Job 9214: indexing and least-squares refinement of powder diffraction data. U.S. Geological Survey Computer Contribution 20.

Bailey, D. K. and Schairer, J. F. (1966) The system Na_2O–Al_2O_3–Fe_2O_3–SiO_2 at 1 atmosphere, and the petrogenesis of alkaline rocks. Journal of Petrology, 7, 114–170.

Bell, K., Dawson, J. B., and Farquhar, R. M. (1973) Strontium isotope studies of alkalic rocks: the active carbonatite volcano Oldoinyo Lengai, Tanzania. Bulletin of the Geological Society of America, 84, 1019–1030.

Bernotat, W. H. and Morteani, G. (1982) The microcline/sanidine transformation isograd in metamorphic regions: Western Tauern Window and Merano-Mules-Antserselva complex (Eastern Alps). American Mineralogist, 67, 43–53.

Blasi, A. (1977) Calculation of T-site occupancies in alkali feldspar from refined lattice constants. Mineralogical Magazine, 41, 525–526.

Brown, G. M. and Vincent, E. A. (1963) Pyroxenes from the late stages of fractionation of the Skaergaard intrusion, East Greenland. Journal of Petrology, 4, 175–197.

Bussen, J. V. and Sakharov, A. S. (1972) Petrology of the Lovozero Alkaline Massif. Nauka, Moscow.

Cameron, M. and Papike, J. J. (1980) Crystal chemistry of silicate pyroxenes. In C. T. Prewitt, Ed., vol. 7, p. 5–92. Reviews in Mineralogy, Mineralogical Society of America, Washington, D. C.

Cermignani, C. and Anderson, G. M. (1983) The plagioclase exchange reaction in carbonate solutions and application to nepheliniza tion. American Journal of Science, 283A, 314–327.

Cooper, A. F., Gittins, J., and Tuttle, O. F. (1975) The system Na_2CO_3–K_2CO_3–$CaCO_3$ at 1 kilobar and its significance in carbonatite petrogenesis. American Journal of Science, 275, 534–560.

Dawson, J. B. (1962) The geology of Oldoinyo Lengai. Bulletin Volcanologique, 24, 349–387.

Dawson, J. B. (1977) Sub-cratonic crust and upper mantle models based on xenolith suites in kimberlite and nephelinitic diatremes. Journal of the Geological Society of London, 134, 173–184.

Dawson, J. B., Bowden, P., and Clark, G. C. (1968) Activity of the carbonatite volcano Oldoinyo Lengai, 1966. Geologische Rundschau, 57, 865–879.

Denaeyer, M. E. (1970) Rapports isotopiques δO et δC et conditions d'affleurement des carbonatites de l'Afrique centrale. Comptes Rendus de l'Académie des Sciences de Paris, 270D, 2155–2158.

Donaldson, C. H., and Dawson, J. B. (1978) Skeletal crystallization and residual glass compositions in a cellular alkali pyroxenite nodule from Oldoinyo Lengai. Implications for evolution of the alkalic carbonatite lavas. Contributions to Mineralogy and Petrology, 67, 139–149.

Gomes, C. de B., Moro, S. L., and Dutra, C. V. (1970) Pyroxenes from the alkaline rocks of Itapirapuã, São Paulo, Brazil. American Mineralogist, 55, 224–230.

Guest, H. J. (1954) The volcanic activity of Oldoinyo L'Engai. Records of the Geological Survey of Tanganyika, 4, 56–59.

Hamilton, D. L. (1961) Nephelines as crystallization temperature indicators. Journal of Geology, 69, 321–329.

Hamilton, D. L., Freestone, I. C., Dawson, J. B., and Donaldson, C. H. (1979) Origin of carbonatites by liquid immiscibility. Nature, 279, 52–54.

Heinrich, E. W. (1966) The Geology of Carbonatites. Rand McNally, Chicago, Illinois.

Kresten, P. and Morogan, V. (1985) Fenitization at the Fen complex, southern Norway, Lithos,

Kroll, H. (1971) Feldspäte im system $KAlSi_3O_8$–$NaAlSi_3O_8$–$CaAl_2Si_2O_8$: Al,Si-Verteilung und Gitterparameter, Phasen-Transformationen und Chemismus. Ph.D. thesis, Westfälichen Wilhelms-Universität, Münster.

Larsen, L. M. (1976) Clinopyroxenes and coexisting mafic min-

erals from the alkaline Ilimaussaq intrusion. Journal of Petrology, 17, 258–290.

Lehtinen, M. and Sahama, T. G. (1981) A note on the feldspars in the granite xenoliths of the Nyiragongo magma. Bulletin Volcanologique, 44, 451–454.

Le Bas, M. J. (1977) Carbonatite–Nephelinite Volcanism. J. Wiley and Sons, London.

Le Bas, M. J. (1980) The East African Cenozoic magmatic province. Atti Accademia nazionale Lincei, 47, 111–122.

Martin, R. F. (1973) Controls of ordering and subsolidus phase relations in the alkali feldspars. In W. S. MacKenzie and J. Zussman, Eds., The Feldspars Proceedings of the NATO Advanced Study Institute, p. 313–336. Manchester University Press, Manchester, England.

Martin, R. F. (1974) The alkali feldspar solvus: the case for a first-order break on the K-limb. Bulletin de la Société française de Minéralogie et de Cristallographie, 97, 346–355.

Mitchell, R. H. (1980) Pyroxenes of the Fen alkaline complex, Norway. American Mineralogist, 65, 45–54.

Morogan, V. (1982) Fenitization und Ultimate Rheomorphism of Xenoliths from the Oldoinyo Lengai Carbonatitic Volcano, Tanzania. M.S. thesis, McGill University, Montreal, Canada.

Nicholls, J., and Carmichael, I. S. E. (1969) Peralkaline acid liquids: a petrological study. Contributions to Mineralogy and Petrology, 20, 268–294.

Nolan, J. (1966) Melting-relations in the system $NaAlSi_3O_8$–$NaAlSiO_4$–$NaFeSi_2O_6$–$CaMgSi_2O_6$–H_2O, and their bearing on the genesis of alkaline undersaturated rocks. Journal of the Geological Society of London, 122, 119–157.

O'Neil, J. R. and Hay, R. L. (1973) $^{18}O/^{16}O$ ratios in cherts associated with the saline lake deposits of East Africa. Earth and Planetary Science Letters, 19, 257–266.

Parsons, I. and Brown, W. L. (1984) Feldspars and the thermal history of igneous rocks. In W. L. Brown, Ed., Feldspar and Feldspathoids: Structures, Properties and Occurrences, p. 317–371. D. Reidel Publishing Company, Dordrecht, Holland.

Perchuk, L. L. and Ryabchikov, I. D. (1968) Mineral equilibria in the system nepheline–alkali feldspar–plagioclase and their petrological significance. Journal of Petrology, 9, 123–167.

Pickering, R. (1961) The geology of the country around Endulen. Records of the Geological Survey of Tanganyika, 11, 1–10.

Powell, M. and Powell, R. (1977) A nepheline–alkali feldspar geothermometer. Contributions to Mineralogy and Petrology, 62, 193–204.

Reck, H. (1914) Oldoinyo Lengai, ein tätiger Vulkan in Gebiete der Deutsch-Ostafrikanischen Bruchstufe. Branca Festschrift, 7, 373–409.

Rubie, D. C. and Gunter, W. D. (1983) The role of speciation in alkaline igneous fluids during fenite metasomatism. Contributions to Mineralogy and Petrology, 82, 165–175.

Stephenson, D. (1972) Alkali clinopyroxenes from nepheline syenites of the South Qôroq Centre, South Greenland. Lithos, 5, 187–201.

Stewart, D. B. and Wright, T. L. (1974) Al/Si order and symmetry of natural alkali feldspars, and the relationship of strained cell parameters to bulk composition. Bulletin de la Société française de Minéralogie et de Cristallographie, 97, 356–377.

Sutherland, D. S. (1965) Potash-trachytes and ultra-potassic rocks associated with the carbonatite complex of the Toror Hills, Uganda. Mineralogical Magazine, 35, 363–378.

Tyler, R. C. and King, B. C. (1967) The pyroxenes of the alkaline igneous complexes of Eastern Uganda. Mineralogical Magazine, 280, 5–22.

Varet, J. (1969) Les pyroxènes des phonolites du Cantal (Auvergne, France). Neues Jahrbuch für Mineralogie Monatshefte, 4, 174–184.

Vinogradov, A. P., Dontsova, E. I., Gerasimovskiy, V. I., and Kuznetsova, L. D. (1971) Oxygen isotopic composition of carbonatites from the rift zones of East Africa. Geochemistry International, 8, 307–313.

von Eckermann, H. (1948) The process of nephelinization. International Geological Congress 18th, 3, 90–93.

Watkinson, D. H. and Wyllie, P. J. (1971) Experimental study of the composition join $NaAlSiO_4$–$CaCO_3$–H_2O and the genesis of alkalic rock–carbonatite complexes. Journal of Petrology, 12, 357–378.

Woolley, A. R. (1969) Some aspects of fenitization with particular reference to Chilwa Island and Kangankunde, Malawi. Bulletin of the British Museum of Natural History (Mineralogy), 2, 189–219.

Wright, T. L. and Doherty, P. C. (1970) A linear programming and least squares computer method for solving petrologic mixing problems. Bulletin of the Geological Society of America, 81, 1995–2008.

Yagi, K. (1953) Petrochemical studies of the alkalic rocks of the Morotu district, Sakhalin. Bulletin of the Geological Society of America, 64, 769–810.

Manuscript received, January 17, 1985;
accepted for publication, July 15, 1985.